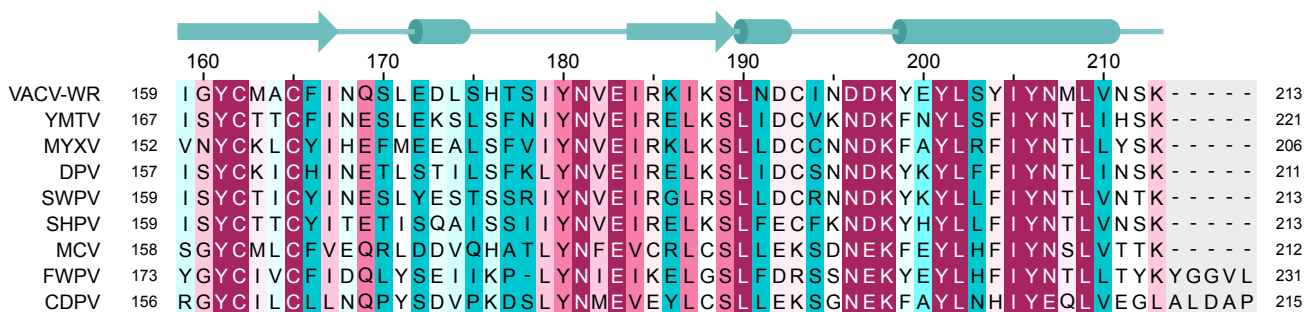
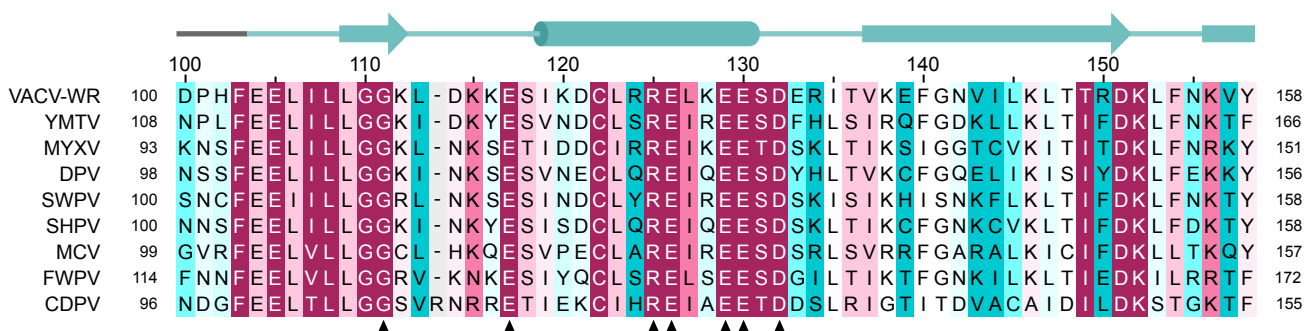
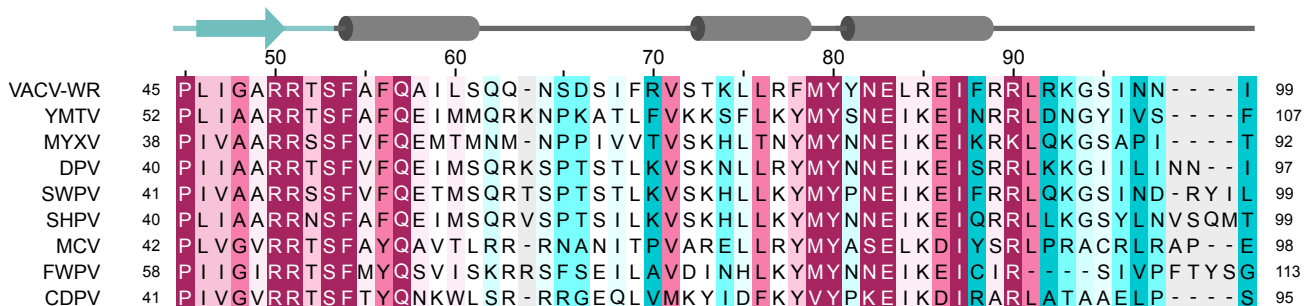
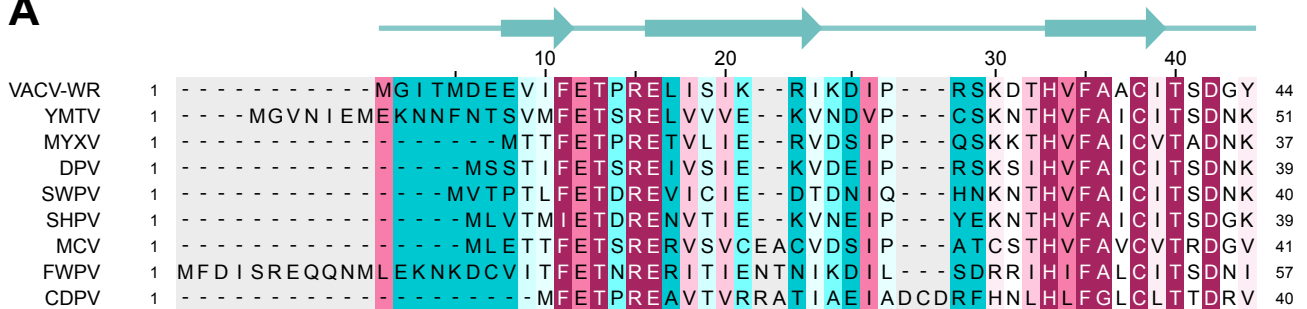
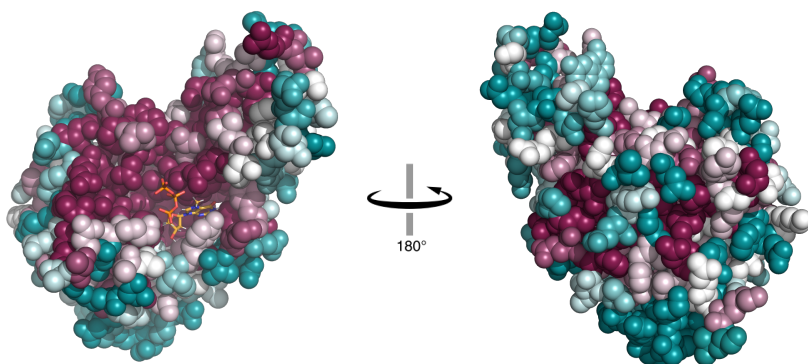


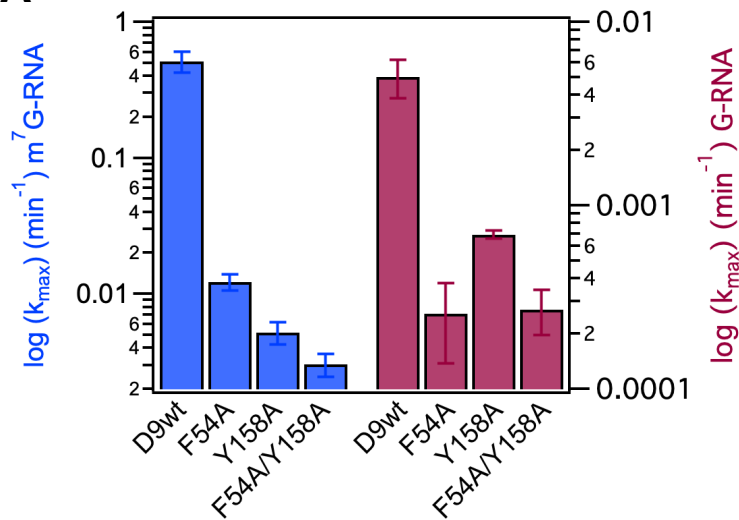
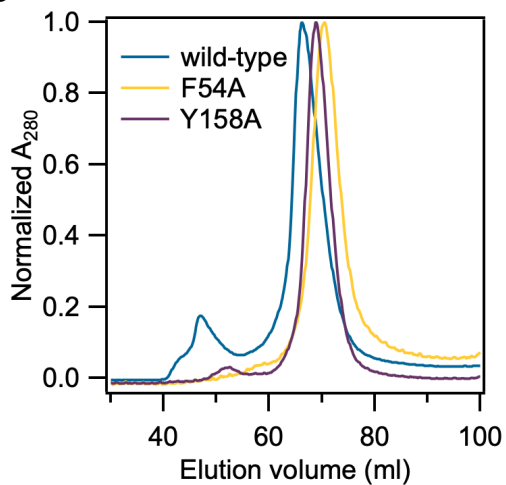
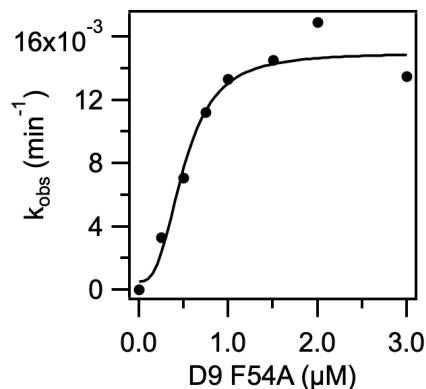
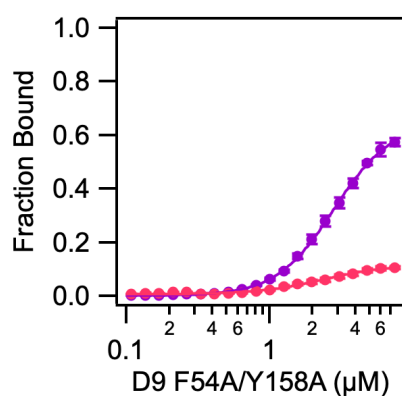
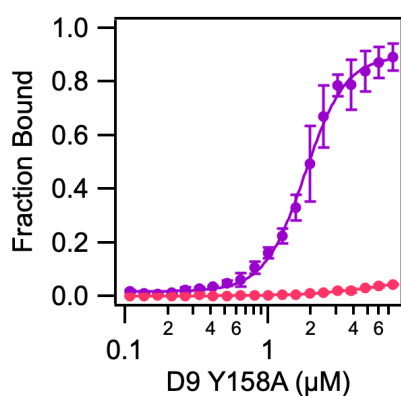
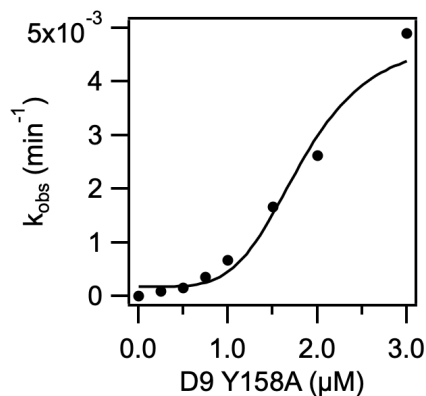
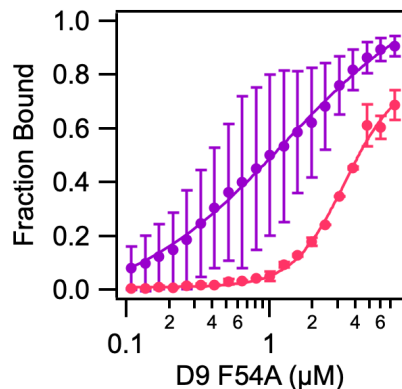
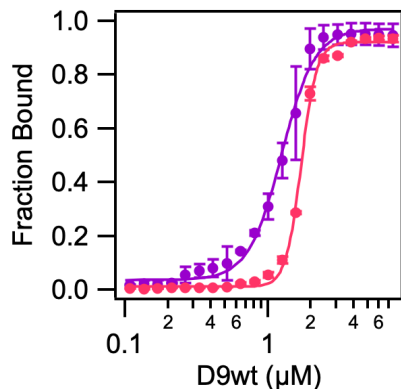
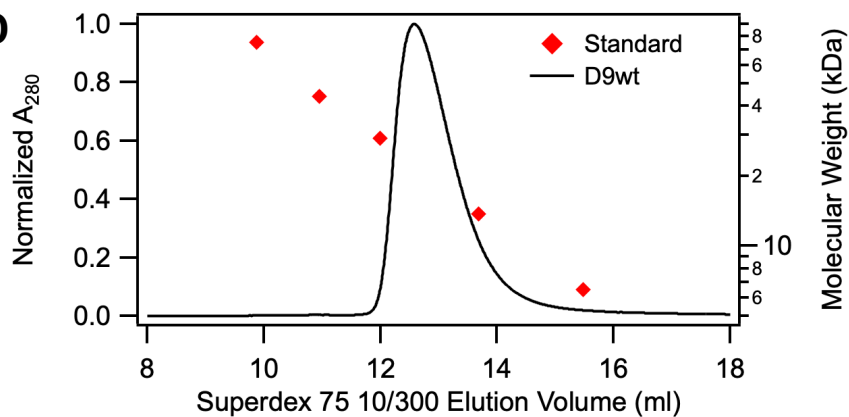
**A**



**B**



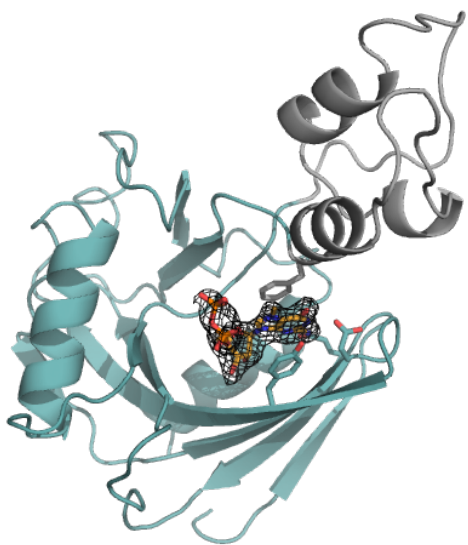
**Figure S1.** Sequence conservation of D9 among chordopoxvirinae, Related to Figure 1. (A) Sequence alignment of representative D9 sequences. VACV-WR, vaccinia virus western reserve strain; YMTV, yaba monkey tumor virus; MYXV, myxoma virus; DPV, deerpox virus; SWPV, swinepox virus; SHPV, sheeppox virus; MCV, molluscum contagiosum virus; FWPV, fowlpox virus; CDPV, crocodylidpox virus. Background color is coded by ConSurf conservation score from variable (teal) to conserved (magenta) from multiple sequence alignment of all available D9 sequences. Numbering above the sequences follows VACV-WR residue number. Secondary structure for VACV is shown above the sequences where arrows are beta sheets and cylinders are alpha helices. Coloring is the same as Figure 1. Triangles below indicate conserved residues in the Nudix motif, consisting of the sequence  $GX_5EX_7REUXEEXGU$ , where X represents any residue and U represents an isoleucine, leucine or valine. (B) 3D structure of product-bound D9 with D9 shown as space-filled model and  $m^7GDP$  shown as sticks. Residues are colored by conservation as in (A).

**A****B****C****E****D**

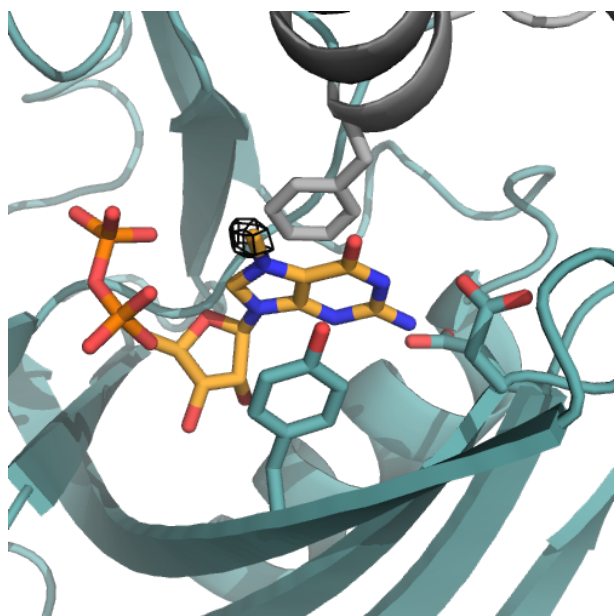
**Figure S2.** Residue Y158 plays multiple roles in substrate binding and catalysis, Related to Figure 2. (A) Bar graph showing the rate of the catalytic step ( $k_{\max}$ ) plotted on a log scale for cap binding mutants using methylated (blue) and unmethylated (purple) RNA substrate. Error is s.e.m. for the rate measured in two independent experiments. (B) Preparative size exclusion chromatography (SEC) of wild-type D9 (blue) and cap binding mutants F54A (yellow) and Y158A (purple) from the final step in their individual purifications (superdex 75 16/600 gel filtration column). Elution volumes are 66.2, 70.4, and 68.9ml, respectively. (C) Graphs of  $k_{\text{obs}}$  versus mutant D9 concentration for decapping of m<sup>7</sup>G-RNA. Each data point is from a single replicate. F54A:  $K_m=0.5\mu\text{M}$ ,  $k_{\max}=0.015\text{min}^{-1}$ ,  $n=2.7$ ; Y158A:  $K_m=1.82\mu\text{M}$ ,  $k_{\max}=0.0048\text{min}^{-1}$ ,  $n=4.6$ . (D) Analytical SEC of wild-type D9 and molecular weight standards aprotinin (6.5 kDa), ribonuclease A (13.7 kDa), carbonic anhydrase (29 kDa), ovalbumin (44 kDa), and conalbumin (75 kDa). The apparent molecular weight of wild-type D9 determined from elution volume comparison to standards is 21.1 kDa. (E) Fraction of RNA bound versus concentration of D9 for m<sup>7</sup>G-capped RNA (purple) and 5' monophosphate RNA (pink) for cap binding mutants F54A, Y158A and F54A/Y158A. The equilibrium dissociation constants and Hill coefficients are shown in Table S2. Error is s.e.m. for the binding measured in two independent experiments.



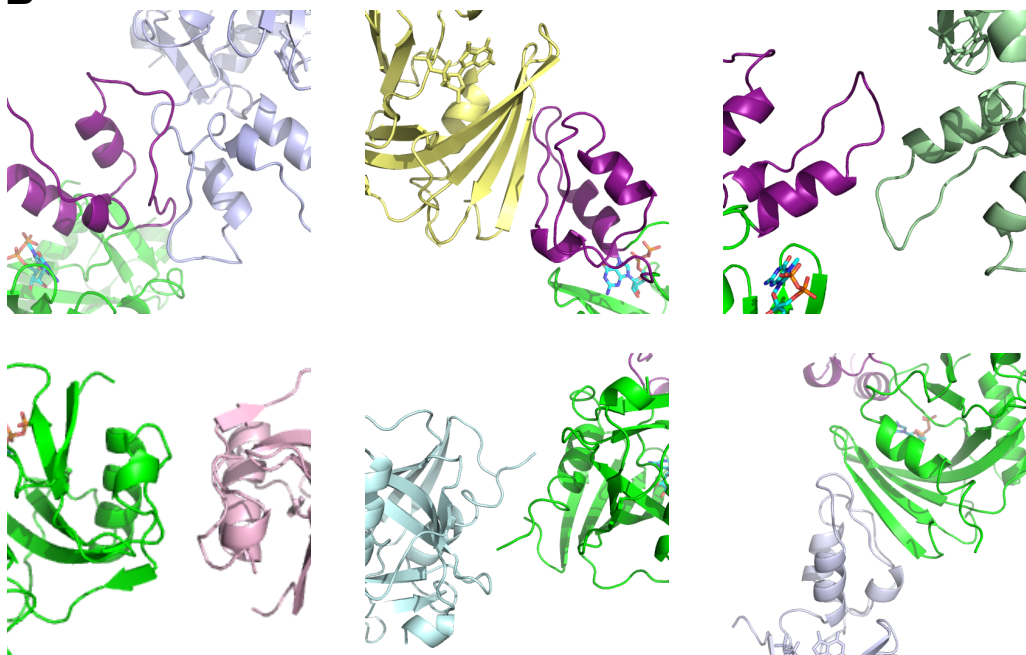
**A**



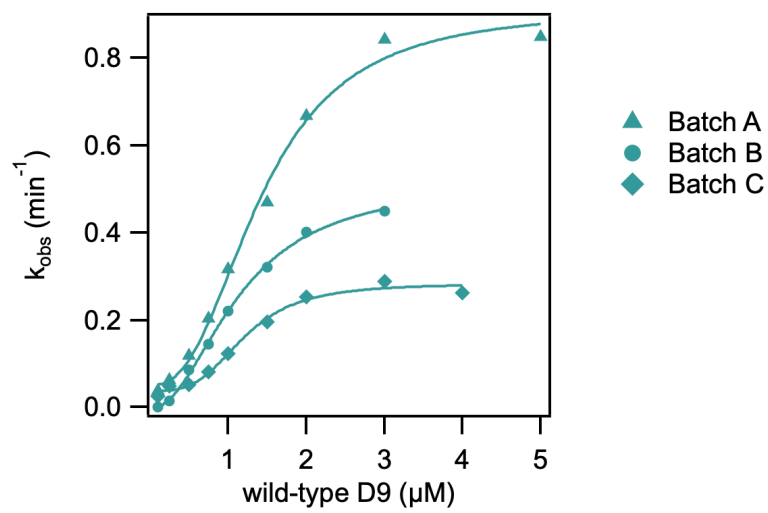
**B**



**Figure S3.** Trinucleotide substrate positioning in cap binding pocket, Related to Figure 3. (A) Crystal structure of VACV-WR D9 bound to non-hydrolyzable trinucleotide substrate (PDB 7SF0).  $F_o-F_c$  omit map is shown for trinucleotide substrate at  $2.0\sigma$ . Only clear density is observed for the  $m^7G$  cap and two phosphate groups. (B) Close up view showing positioning of the  $m^7G$  cap between aromatic residues F54 and Y158.  $F_o-F_c$  omit map is shown for the N7-methyl moiety at  $3.5\sigma$ .

**A****B**

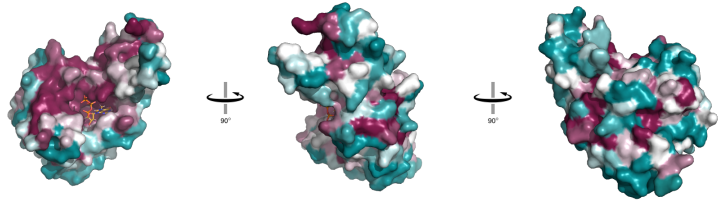
**Figure S4.** Crystal packing observed in PDB 7SEZ, Related to Figures 2, 4, 5 and Table 2. (A) The asymmetric unit is shown as green (Nudix domain) and purple (insertion domain) with symmetry mates depicted in pale shades. (B) Close up view of the 6 contacts the asymmetric unit makes with neighboring symmetry mates.

**A****B**

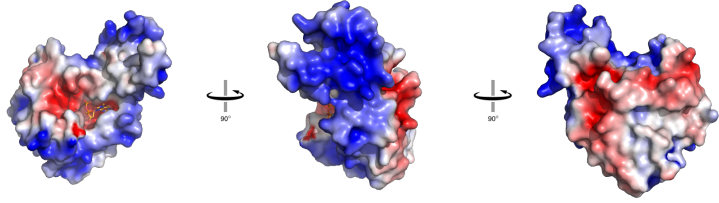
Preparation	$K_m$ (μM)	$k_{max}$ (min <sup>-1</sup> )	Hill coefficient
Batch A	$1.42 \pm 0.092$	$0.912 \pm 0.044$	2.5
Batch B	$1.16 \pm 0.061$	$0.517 \pm 0.023$	2.0
Batch C	$1.21 \pm 0.080$	$0.284 \pm 0.013$	3.4

**Figure S5.** Measured decapping rate is variable between different RNA preparations, Related to Figure 5 and table 2. (A) Graph of  $k_{\text{obs}}$  versus wild-type D9 concentration for three different preparations of m<sup>7</sup>G capped 29nt RNA substrate. (B) Fitted  $K_M$ ,  $k_{\text{max}}$  and Hill coefficient values for data in (A). Errors are the standard error from the obtained fits to equation 1.

**Conservation**



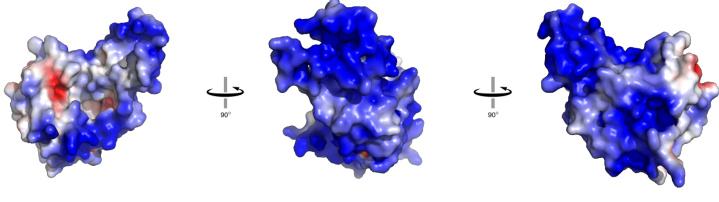
**VACV-WR**



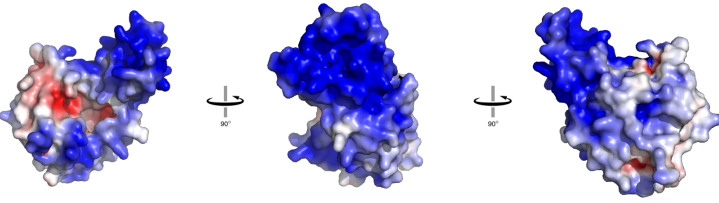
**YMTV**



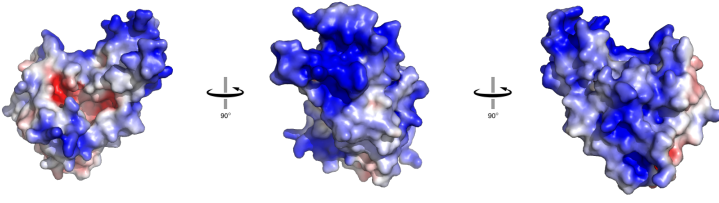
**MYXV**



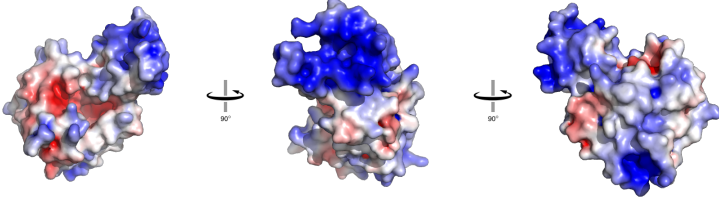
**DPV**



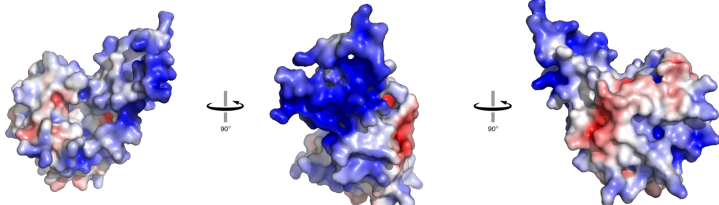
**SWPV**



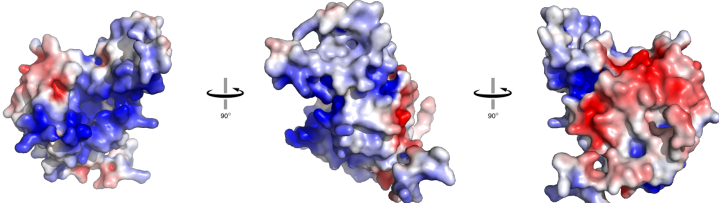
**SHPV**



**MCV**



**FWPV**



**CDPV**

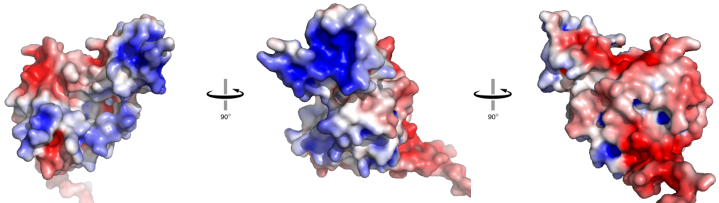


**Figure S6.** D9 electrostatic surface comparison of representative poxviruses, Related to Figure 5. Poxvirus sequences from eight different genera were modelled onto the D9 crystal structure (PDB 7SEZ) using MODELLER (Šali and Blundell, 1993) using sequence alignments generated using MUSCLE (Madeira et al., 2019). Electrostatic surfaces shown are -5 to +5 kT/e. Top row is sequence conservation as determined by Consurf server using multiple sequence alignment of all known D9 sequences (Figure S1).



Table S1. Substrate binding affinities measured by filter binding assay, Related to Figures 4 and 5.

D9 construct	RNA	$K_d$ ( $\mu$ M)	Hill Coefficient
wt	m <sup>7</sup> G-GN <sub>28</sub>	1.25	3.7
	G-GN <sub>28</sub>	1.56	4.2
	m <sup>7</sup> G-AN <sub>28</sub>	1.41	6.4
	m <sup>7</sup> G-m <sup>6</sup> AN <sub>28</sub>	1.27	3.7
	p-GN <sub>28</sub>	1.71	8.08
	5' overhang dsRNA	0.87	6.0
	Blunt end dsRNA	1.32	9.0
	3' overhang dsRNA	1.29	10.3
F54A	m <sup>7</sup> G-GN <sub>28</sub>	1.28	0.78
	p-GN <sub>28</sub>	3.37	2.38
Y158A	m <sup>7</sup> G-GN <sub>28</sub>	1.82	3.04
	p-GN <sub>28</sub>	n.b. <sup>a</sup>	-
F54A/Y158A	m <sup>7</sup> G-GN <sub>28</sub>	2.82	2.17
	p-GN <sub>28</sub>	n.b. <sup>a</sup>	-

<sup>a</sup>Binding affinities could not be determined for lack of sufficient binding at highest protein concentration.

Table S2. RNA sequences used for activity and binding assays, Related to STAR Method Details (Kinetic decapping assays, Filter binding assays).

Name	RNA sequence
GN <sub>28</sub>	GGGCAGAUUACAGCACGACAUAACACUAA (29) <sup>a</sup>
AN <sub>28</sub>	AGGCAGAUUACAGCACGACAUAACACUAA (29)
m <sup>6</sup> AN <sub>28</sub>	m <sup>6</sup> AGGCAGAUUACAGCACGACAUAACACUAA (29)
5' overhang AS RNA	<b>GGGUUAGUGUUAUGUCGUGCUG</b> (22)
Blunt capped end AS RNA	<b>GGGUUAGUGUUAUGUCGUGCUGUAAUCUGCCC</b> (32)
3' overhang AS RNA	<b>GGGUUAGUGUUAUGUCGUGCUGUAAUCUGCCCCAAUAAUACC</b> (42)

<sup>a</sup>Values in parentheses denote RNA length. Nucleotides in bold do not anneal to complementary RNA (GN<sub>28</sub>) in dsRNA constructs.